Research Article | Vol. 27, No. 8 | 15 Apr 2019 | OPTICS EXPRESS 11303
Optics EXPRESS

Performance of free-space optical communication systems: effect of aerosol-induced lower atmospheric warming

K. SUNILKUMAR,[1,2,*] N. ANAND,[1,3] S. K. SATHEESH,[1,3] K. KRISHNA MOORTHY,[1] AND G. ILAVAZHAGAN[2]

[1]*Centre for Atmospheric and Oceanic Sciences, Indian Institute of Science, Bengaluru, India*
[2]*Centre for Photonics and LIDAR Research, Hindustan Institute of Technology and Science, Chennai, India*
[3]*Divecha Centre for Climate Change, Indian Institute of Science, Bengaluru, India*
**sunilkumark@iisc.ac.in*

Abstract: We report the effect of aerosol-induced local atmospheric heating and the resulting changes in the lower atmospheric optical turbulence on the performance of Free-Space Optical (FSO) communication links. A closed form mathematical expression is derived to estimate the influence of aerosol-induced warming on the Bit Error Rate (BER) of a Binary Phase Shift Keying FSO communication link through Gamma-Gamma modeled turbulence. Our results demonstrate a strong impact, with the aerosol-induced turbulence taking a toll on the signal-to-noise ratio of ~20 dB for a BER of 10^{-9}. Aerosol-induced warming produces significant variations in BER compared to the clear atmospheric conditions and can subdue the benefits of improved beam alignment.

1. Introduction

Free Space Optical (FSO) communication is a line of sight technology, where data laden optical signals propagate through the atmosphere characterized by fluctuations in the thermo-dynamical properties such as temperature, pressure and wind velocity and direction etc., superposed on the regular variations [1]. These random fluctuations cause wave-front distortion and signal degradation at the receiver. Continuously varying nature of the signal - both temporally and spatially - makes the retrieval of information more difficult. Wave front distortion of laser beam propagating through the atmosphere has been studied extensively and reported to have limiting effects on the performance of communication systems [2–5]. Such distortions arise due to the interaction of the wave front with (a) thermal eddies and (b) gas molecules and suspended particles (aerosols) in the atmosphere. Random fluctuations in the intensity of a beam propagating through the atmospheric turbulence are quantified by the refractive index structure parameter (C_n^2). Several models are in use to estimate clear air optical turbulence [6]. Recent studies on the modulation of C_n^2 due to variations in the atmospheric residence time and vertical distribution of aerosols [7,8] have clearly quantified the aerosol-induced optical scintillations through absorption, scattering and radiative effects, when they are present close to the surface or in the elevated layers [9] of the Earth's lower atmosphere (troposphere). Extinction effects of aerosols on optical turbulence [10–12] and FSO communication links [5,13,14] were reported earlier. Commonly used intensity fluctuation models [6] neglect the heating effects of absorbing atmospheric aerosols (such as black carbon and dust, which strongly absorb in the visible through near infra-red wavelengths of the incident solar energy). Hence, the modulation of atmospheric C_n^2 by aerosol-induced warming and its consequence on FSO communication systems have not been investigated extensively. Under this backdrop, the present work focuses on the radiative

#351121 https://doi.org/10.1364/OE.27.011303
Journal © 2019 Received 5 Nov 2018; revised 19 Dec 2018; accepted 20 Dec 2018; published 9 Apr 2019

Optics EXPRESS

effects of atmospheric aerosols and its consequence on the Bit Error Rate (BER) performance of FSO communication systems.

2. System and channel model

In order to improve the information transfer through the stochastic atmosphere, various signal as well receiver design techniques have been proposed and adopted in communication engineering community over the years. Among the signal design techniques, modulating the information in different ways to the carrier signal amplitude, phase and frequency were attractive due its efficient resilience to channel induced impairments. Traditionally ON-OFF Keying (OOK) is the most attractive due to its simple modulation process and less complex receiver design. Carrier phase modulated systems offer better performance over OOK, though receiver design is complex. We report the effects of lower-tropospheric aerosol-induced warming on the BER performance of binary phase shift keying (BPSK) coherent heterodyne FSO communication systems under Kolmogorov turbulence. Even though anisotropic turbulence (non-Kolmogorov) prevails in the atmosphere, it is reasonable to assume isotropic turbulence in the lower atmosphere [15,16]. The received signal can be represented as [3]:

$$y = Ix + n \tag{1}$$

where 'y' is the received signal, 'I' the channel state, 'x' the transmitted signal and 'n' the signal independent additive white Gaussian noise with variance σ_n^2. The randomly varying channel state is assumed to be the product of three independent factors which can be formulated as:

$$I = I_l I_p I_s \tag{2}$$

where I_l, I_p and I_S are the path loss, pointing errors and fading due to atmospheric turbulence respectively. We model the intensity fluctuations due to thermal eddies in the atmosphere, generated by aerosol-induced warming, using the well-known Gamma-Gamma model. These intensity fluctuations are characterized by Rytov variance and are given for plane waves as [2]:

$$\sigma_R^2 = 1.23 C_n^2 k^{7/6} L^{11/6} \tag{3}$$

where 'k' is the wave number and 'L' is the link length. We represent C_n^2 as the refractive index structure parameter calculated using the unperturbed atmospheric data and C_n^{2*} as the same when perturbed by the radiative effects of the aerosol fields.

3. Coherent systems

Coherent system photo detection circuits operate on the combined data laden optical signal and a locally generated optical signal to generate an intermediate frequency before it is band pass filtered for electronic processing to retrieve the transmitted information. The alternating current component I_{ac} (t), after band pass filtering, is given by [17]:

$$I_{ac}(t) = R(P_S + P_{LO}) + 2R\sqrt{P_S P_{LO}} \cos(\omega_{IF} t + \phi_S - \phi_{LO}) \tag{4}$$

where P_S is the received optical signal power, P_{LO} is the local oscillator signal power, R represents the photodetector responsivity, ω_{IF} is the intermediate frequency after heterodyning the incoming and local oscillator signals and ϕ_S and ϕ_{LO} represent the signal and local oscillator phases respectively. In practice, $P_s << P_{LO}$ and the dc term can be filtered to obtain the ac component as:

$$I_{ac}(t) = 2R\sqrt{P_S P_{LO}} \cos(\omega_{IF} t + \phi_S - \phi_{LO}) \tag{5}$$

Optics EXPRESS

The signal to noise ratio (SNR) can be obtained by dividing the average signal power by the average noise power and is given by:

$$SNR = \frac{\langle I_{ac} \rangle^2}{\sigma^2} \tag{6}$$

where variance σ^2 is the sum of shot noise and thermal noise current fluctuations and the angular brackets indicate the averaged values. Hence the SNR for a coherent heterodyne system can be written as [17]:

$$SNR = \frac{2R^2 \overline{P_S} P_{LO}}{2q(RP_{LO} + I_d)\Delta f + \sigma_T^2} \tag{7}$$

where q is the electron charge, I_d is the dark current, Δf is the effective noise equivalent bandwidth of the receiver, $\overline{P_s}$ is the average received optical power and σ_T^2 the thermal noise variance. The receiver P_{LO} can be made sufficiently large so that $\sigma_T^2 << \sigma_S^2$ (shot noise variance), and the SNR can be approximated as:

$$SNR = \frac{R\overline{P_S}}{q\Delta f} \tag{8}$$

The conditional BER for a coherent BPSK system is given by [18]:

$$P_e(I_S) = Q(\sqrt{I_S \bar{\gamma}}) \tag{9}$$

where I_S is the instantaneous irradiance of the received optical signal, $\bar{\gamma}$ is the average SNR and Q is the Gaussian Q function which can be represented in terms of the complimentary error function. Thus,

$$Q(\sqrt{I_S \bar{\gamma}}) = \frac{1}{2} erfc(\sqrt{\frac{I_S \bar{\gamma}}{2}}) \tag{10}$$

We choose a Gamma-Gamma model for the intensity fluctuations (I_s), which efficiently represents the turbulence induced intensity variations over weak to strong regimes. The probability density function (PDF) of intensity fluctuations is given as [18]:

$$f_{I_S}(I_S) = \frac{2(\alpha\beta)^{(\alpha+\beta)/2}}{\Gamma(\alpha)\Gamma(\beta)} (I_S)^{(\alpha+\beta/2)-1} K_{\alpha-\beta}(2\sqrt{\alpha\beta I_S}) \text{ for } I_S>0 \tag{11}$$

where α and β are the effective number of small-scale eddies (eddies smaller than the first Fresnel zone or coherence radius) and large-scale eddies (eddies larger than the first Fresnel zone), K_υ denotes the υ^{th} order modified Bessel's function of the second kind. Thus, the average BER is:

$$\overline{P_b}(e) = \int_0^\infty P_e(I_S) f_{I_S}(I_S) dI_S \tag{12}$$

Niu et al. employed an alternate form of Q function [18] to estimate the BER for coherent FSO communication systems through clear air turbulence without considering the pointing error and beam displacement effects. By incorporating the signal fading due to beam pointing errors, Eq. (11) can be rewritten as [4, eqn. 9]:

Optics EXPRESS

$$f_I(I)=\frac{2\gamma^2(\alpha\beta)^{(\alpha+\beta)/2}}{(A_0I_l)^{\gamma^2}\Gamma(\alpha)\Gamma(\beta)}I^{\gamma^2-1}\int_{I/A_0I_l}^{\infty}(I_S)^{(\alpha+\beta/2)-\gamma^2-1}K_{\alpha-\beta}(2\sqrt{\alpha\beta I_S})dI_S \text{ for } I_S>0 \quad (13)$$

Equation (12) for average BER can be rewritten by using Eq. (10) and (13) as:

$$\overline{P_b}(e)=\frac{1}{2}\int_0^{\infty}erfc\left(\sqrt{\frac{I_S\bar{\gamma}}{2}}\right)dI_S\int_{I/A_0I_l}^{\infty}I^{\gamma^2-1}\frac{2\gamma^2(\alpha\beta)^{(\alpha+\beta)/2}}{(A_0I_l)^{\gamma^2}\Gamma(\alpha)\Gamma(\beta)}(I_S)^{(\alpha+\beta/2)-\gamma^2-1}K_{\alpha-\beta}(2\sqrt{\alpha\beta I_S})dI_S \quad (14)$$

A direct integration of the above expression is cumbersome and expressing the functions in terms of Meijer's G function [4] will result into inconsistent solutions for numerical evaluation. We therefore write the average BER as below [19]:

$$\overline{P_b}(e)=-\int_0^{\infty}P_e'(I_S)F_{I_S}(I_S)dI_S \quad (15)$$

where, $F_{I_S}(I_S)$ is the cumulative distribution function (CDF) of the intensity fluctuations under Gamma-Gamma distribution with pointing errors given by [4]:

$$F_{I_S}(I_S)=\frac{\gamma^2}{\Gamma(\alpha)\Gamma(\beta)}G_{2,4}^{3,1}\left[\frac{\alpha\beta I_S}{A_0I_l}\middle|\begin{matrix}1 & \gamma^2+1\\ \gamma^2 & \alpha\quad\beta\quad 0\end{matrix}\right] \quad (16)$$

where G indicates the Meijer's G function, γ is the ratio of equivalent beamwidth to standard deviation of the pointing error displacement. $P_e'(I_S)$ can be obtained by differentiating Eq. (10). This can be done using the identity given in [20]. Thus,

$$P_e'(I_S)=\frac{-1}{\sqrt{\pi}}\exp\left(\frac{-I_S\bar{\gamma}}{2}\right) \quad (17)$$

Substituting Eqs. (16) and (17) in Eq. (15) gives,

$$\overline{P_b}(e)=\frac{\gamma^2}{\sqrt{\pi}\Gamma(\alpha)\Gamma(\beta)}\int_0^{\infty}\exp\left(\frac{-I_S\bar{\gamma}}{2}\right)G_{2,4}^{3,1}\left[\frac{\alpha\beta I_S}{A_0I_l}\middle|\begin{matrix}1 & \gamma^2+1\\ \gamma^2 & \alpha\quad\beta\quad 0\end{matrix}\right]dI_S \quad (18)$$

Using the Laplace transform of Meijer's G function [21, eqn. 5.6.3 (1)], Eq. (18) can be solved as

$$\overline{P_b}(e)=\frac{2\gamma^2}{\bar{\gamma}\sqrt{\pi}\Gamma(\alpha)\Gamma(\beta)}G_{3,4}^{3,2}\left[\frac{2\alpha\beta}{A_0I_l\bar{\gamma}}\middle|\begin{matrix}0 & 1 & \gamma^2+1\\ \gamma^2 & \alpha & \beta\quad 0\end{matrix}\right] \quad (19)$$

Thus Eq. (19) gives the closed form expression for average BER of coherent BPSK system with pointing errors, where Meijer's G function can be calculated using software package Mathematica.

4. Materials and methodology for estimating aerosol radiative effects

The basic theory of radiative transfer through plain parallel atmosphere has been provided by the classic work of Chandrasekhar [22]. Based on this, the radiative effects of atmospheric aerosols have been extensively reviewed [23] and experimentally investigated by several investigators [24–26]. Various methods have been proposed to obtain the solution of the relevant integro-differential equation which governs the radiative transfer of energy in a plane parallel atmosphere [27]. Among them, the phase function expansion using Legendre polynomials is employed in several widely used Radiative Transfer codes such as

Optics EXPRESS

LOWTRAN and MODTRAN. The discrete ordinate method developed by Chandrasekhar is affirmed to be a powerful method to estimate the radiation transfer through aerosols and clouds. The Santa Barbara Discrete Ordinate Radiative Transfer (SBDART) code [28] developed and used by atmospheric science community employs discrete ordinate technique where the radiative transfer equation is discretized, and solutions are obtained for a set of differential equations. Since the suspended atmospheric aerosols are of size comparable with the wavelength of operation of FSO communication systems, scattering and absorption of radiation are predominant in this spectrum and for which discrete ordinate method is proven to be an efficient technique [27].

Aerosol Optical Depth (AOD), an important parameter denoting the columnar loading of atmospheric aerosols, obtained from Moderate Resolution Imaging Spectroradiometer (MODIS) onboard TERRA satellite, along with the optical properties of aerosols (continental polluted model) taken from a Mie scattering model (Optical Properties of Aerosols and Clouds - OPAC) [29] have been used in our work to input realistic aerosol fields to Santa Barbara DISORT Atmospheric Radiative Transfer (SBDART) model [28]. Meteorological profiles from GPS radiosonde observations, multispectral surface albedo obtained from MODIS–TERRA and CALIOP (Cloud-Aerosol Lidar with Orthogonal Polarization) lidar derived aerosol extinction profiles also formed as input to SBDART. The study was carried out over a semi-arid region near an urban location Hyderabad in India (13.5° N, 79.2° E) over winter (December to February, DJF), pre-monsoon (March to May, MAM), monsoon (June to September, JJAS) and post-monsoon (October to November, ON) seasons.

With a view to examining the radiative effects of atmospheric aerosols on the performance of FSO communication systems, aerosol parameters were perturbed following the method described in [7,8]. Long-term (2006 to 2012) averaged level 3 seasonal AOD values of 0.27, 0.34, 0.29 and 0.33 for DJF, MAM, JJAS and ON seasons and an aerosol residence time of one day were taken in the present study. Table 1 shows the estimated vertically averaged values of C_n^2, C_n^{2*} and $d^2T/dtdz$, where C_n^2 is the refractive index structure parameter calculated using the unperturbed atmospheric data, C_n^{2*} is the same when radiative effects of perturbed aerosol fields are also incorporated and $d^2T/dtdz$ is the vertical gradient of aerosol-induced atmospheric heating rate. $d^2T/dtdz$ (a signature of vertical distribution of aerosols) influences the perturbations in C_n^2 significantly compared to AOD (a signature of total aerosol columnar loading) as reported in [7]. Higher the value of $d^2T/dtdz$, higher the vertical temperature gradient, thereby resulting in higher C_n^2 values. The competing effects of the aerosol parameters (AOD and $d^2T/dtdz$) are explained in the numerical results. Large increase in C_n^2 (about two orders of magnitude) is visible when radiative effects of perturbed aerosol fields are introduced.

Table 1. Seasonal variations in refractive index structure parameter under unperturbed (C_n^2) and perturbed (C_n^{2*}) conditions

Season	C_n^2 ($m^{-2/3}$)	$d^2T/dtdz$ (K day^{-1} m^{-1})	C_n^{2*} ($m^{-2/3}$)	σ_R^2	σ_R^{2*}
DJF	2.5×10^{-15}	0.225	4.5×10^{-13}	0.35	64.35
MAM	1.5×10^{-15}	0.267	2.9×10^{-13}	0.21	41.71
JJAS	2.9×10^{-15}	0.229	4.3×10^{-13}	0.41	61.49
ON	3.5×10^{-15}	0.349	9.3×10^{-13}	0.50	132.99

5. Numerical calculations

We have numerically estimated the BER of the system discussed above using Eq. (19), for a link-length L = 2000 m and wavelength $\lambda = 0.85$ μm, across all the seasons reported in Table 1. Rytov variance for DJF, MAM, JJAS and ON seasons were calculated for values of C_n^2 due to unperturbed state of the model atmosphere and C_n^{2*} due to perturbed states of aerosol concentrations. These values were employed to estimate the parameters α and β. Pointing

Optics EXPRESS

error statistics of normalized beamwidth $w_z/r = 7.2$ and 6.5 and normalized jitter $\sigma_s/r = 2$ and 0.1 were used to calculate the BER performance of the system.

A set of overlapping curves for perturbed conditions and distinct, seasonal curves for unperturbed conditions are obtained as shown in Fig. 1. The curves show a large increase in the average BER, due to perturbation by aerosols, compared to the unperturbed conditions. It is also interesting to note that while the model atmosphere, without considering the aerosol-induced atmospheric warming, show significant seasonality with a better performance during MAM, the link performance does not show any conspicuous seasonality once the aerosol-induced perturbations are also considered. A large shift in BER marked by reduced slope of the BER curves in the perturbed aerosol state is attributed to the aerosol-induced local warming and subsequent scintillations. This dependence is evident in refractive index variations given in Table 1.

We consider the lowest and highest values of C_n^2 and C_n^{2*} across all seasons (as given in Table 1) for extreme cases analysis. Minimum C_n^2 and C_n^{2*} values are observed in MAM (Fig. 1(b)) and maximum in ON (Fig. 1(d)) seasons. For unperturbed conditions with normalized beamwidth $w_z/r = 7.2$ and normalized jitter $\sigma_s/r = 0.1$, Figs. 1(b) and 1(d) show a BER difference of about four orders of magnitude at 45 dB SNR. When aerosol perturbations are also considered, though these seasonal variations become insignificant, there is a severe degradation in the link performance, with the BER increasing by nearly 8 orders of magnitude in all seasons compared to the unperturbed conditions, showing that aerosol-induced strong turbulence can severely affect the system performance. It can be further observed that under weak turbulence conditions, a small change in w_z/r and σ_s/r results in large difference in BER, but a corresponding change under strong turbulence regimes does not contribute a significant BER change. Thus, large concentration of aerosols residing over long duration can significantly change the performance of FSO links eliminating the possibility of improving the system performance by varying the pointing error statistics.

Identical BER values during DJF and JJAS seasons in Figs. 1(a) and 1(c) are attributed to the similar C_n^2 and aerosol parameters (AOD and $d^2T/dtdz$) prevailing during those seasons, which eventually leads to similar σ_R^2. The aerosol loading is low in these seasons, as are evident from the AOD observations. Nevertheless, similar AOD values do not lead to same BER performance due to the notable difference in C_n^2 and $d^2T/dtdz$ during those two seasons, as can be observed from Table 1. This corroborates the significant dependence of FSO system performance on the perturbations in aerosol parameters, especially $d^2T/dtdz$, and how the coupled effects of aerosols and C_n^2 regulate it. Furthermore, for a fixed BER of 10^{-9}, perturbations in aerosol parameters result in ~20 dB penalty in SNR for all seasons. Thus, the presence of absorbing aerosols not only deteriorates the BER performance, but also necessitates higher SNR in FSO links. It can be observed from the BER curves of all seasons that working on the beamwidth and beam alignment can help in improving the BER under unperturbed conditions but not under the perturbed conditions. It is further noticed that, under perturbed conditions, even a normalized standard deviation of 0.1 for the beam displacement error do not improve the system performance. This is due to the large signal fluctuations produced by aerosol radiative heating.

Optics EXPRESS

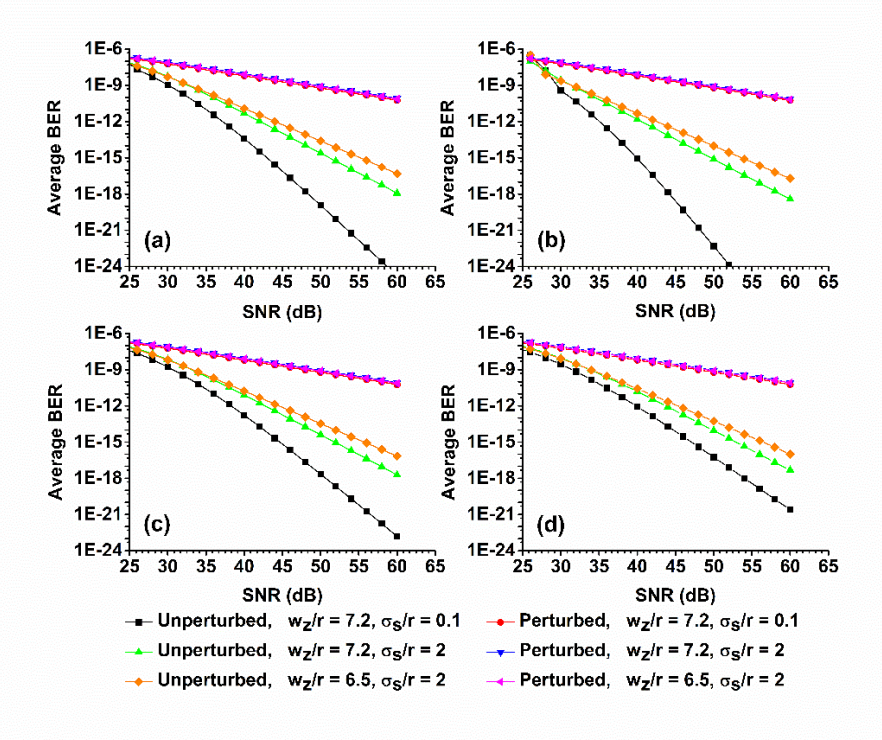

Fig. 1. Average BER plotted against SNR (dB) for unperturbed and perturbed aerosol conditions for (a) DJF, (b) MAM, (c) JJAS and (d) ON seasons.

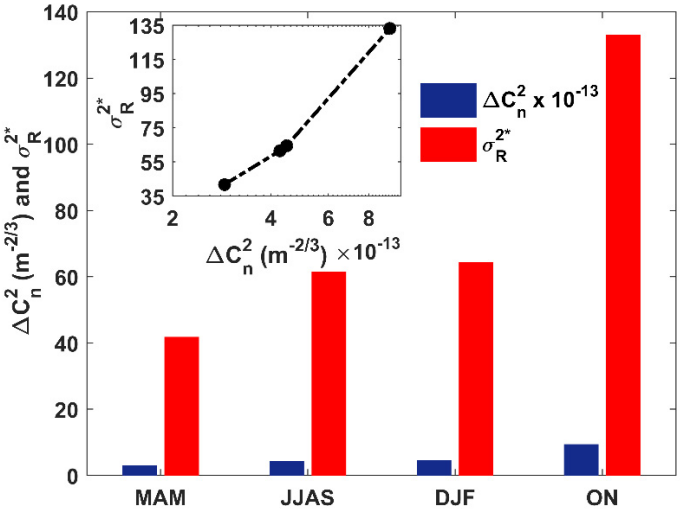

Fig. 2. Dependence of perturbed Rytov variance (σ_R^{2*}) on the perturbations in refractive index structure parameter, $\Delta C_n^2(m^{-2/3})$: seasonal variations (bar diagram) and their relationship (inset).

Dependence of perturbed Rytov variance (σ_R^{2*}) on the perturbations in refractive index structure parameter $\Delta C_n^2 = |C_n^2 - C_n^{2*}|$ is given in Fig. 2. Bar diagram shows the seasonal variations in ΔC_n^2 and σ_R^{2*}, and their corresponding relationship is given in the inset. It is

Optics EXPRESS

clearly observable from Fig. 2 that increase in ΔC_n^2 induced by increasing perturbations in aerosol heating lead to increase in Rytov variance. This strong dependence can also be observed in the BER variations plotted in Fig. 1. We conclude that the aerosol fields and its local warming effects indicated by ΔC_n^2 produces significant variation in BER compared to the clear atmospheric conditions and can subdue the system performance improvement realised through the pointing error statistics.

6. Conclusion

Within the framework of extensive satellite data analysis and a newly derived mathematical expression, we have studied the radiative effects of atmospheric aerosols on the BER performance of a coherent BPSK FSO communication system with pointing errors. Multi satellite and in situ measurements of aerosols and atmospheric parameters show that aerosols can induce strong levels of turbulence locally, when they reside over longer duration in larger concentrations in the atmosphere. Seasonal variation of BER performance is visibly large under unperturbed conditions whereas, there is no significant seasonal variation for perturbed aerosols conditions. This independence helps in system design with specific design parameters along with the spatial and temporal distribution information of aerosols in the atmosphere. It is further noted that reducing the pointing error induced impairments do not contribute much to BER improvement under strong aerosol-induced warming conditions. Our results emphasize the need for inclusion of the radiative effects of atmospheric aerosols during link budget estimation and performance analysis of FSO communication systems.

Funding

Divecha Centre for Climate Change, Indian Institute of Science (IISc).

Acknowledgments

We thank Divecha Centre for Climate Change, Indian Institute of Science (IISc), for supporting this work. We acknowledge the use of high-resolution GPS radiosonde data provided by NARL through www.narl.gov.in. The CALIPSO data were obtained from the NASA Langley Research Center Atmospheric Science Data Center (ASDC) through https://eosweb.larc.nasa.gov. MODIS level 2 albedo was acquired from https:ladsweb.nasacom.nasa.gov. We acknowledge the MODIS mission scientists and associated NASA personnel for the level 3 AOD data used in this work. Anand acknowledges the Grantham fellowship awarded by the Divecha Centre for Climate Change.

References

1. M. Uysal, C. Capsoni, Z. Ghassemlooy, A. Boucouvalas, and E. Udvary, *Optical Wireless Communications Signals and Communication Technology* (Springer, 2016).
2. L. C. Andrews and R. L. Phillips, *Laser Beam Propagation Through Random Media* (SPIE, 2005).
3. H. E. Nistazakis, E. A. Karagianni, A. D. Tsigopoulos, M. E. Fafalios, and G. S. Tombras, ""Average capacity of optical wireless communication systems over atmospheric turbulence channels," IEEE/OSA," J. Lightwave Technol. **27**(8), 974–979 (2009).
4. H. G. Sandalidis, T. A. Tsiftsis, and G. K. Karagiannidis, "Optical wireless communications with heterodyne detection over turbulence channels with pointing errors," IEEE/OSA. J. Lightwave Technol. **27**(20), 4440–4445 (2009).
5. K. Sunilkumar, S. K. Satheesh, G. Ilavazhagan, and K. K. Moorthy, "Free space optical communication system through turbid media with pointing errors," in Proceeding of Imaging and Applied Optics, LS & C (Optical Society of America, 2018).
6. L. C. Andrews, R. L. Phillips, and C. Y. Hopen, *Laser Beam Scintillation with Applications* (SPIE, 2001).
7. N. Anand, S. K. Satheesh, and K. K. Moorthy, "Dependence of atmospheric refractive index structure parameter (C_n^2) on the residence time and vertical distribution of aerosols," Opt. Lett. **42**(14), 2714–2717 (2017).
8. N. Anand, S. K. Satheesh, and K. K. Moorthy, "Modulation of optical turbulence by atmospheric aerosols: influence of vertical distribution and residence time," in Proceeding of Imaging and Applied Optics Congress (pcAOP), (Optical Society of America, 2018).
9. N. Anand, K. Sunilkumar, S. K. Satheesh, and K. K. Moorthy, "Distinctive roles of elevated absorbing aerosol layers on free-space optical communication systems," Appl. Opt. **57**(25), 7152–7158 (2018).

Optics EXPRESS

10. D. Sadot and N. S. Kopeika, "Forecasting optical turbulence strength on basis of macroscale meteorology and aerosols: models and validation," Opt. Eng. **31**(2), 200–212 (1992).
11. N. S. Kopeika, *A System Engineering Approach to Imaging* (SPIE Optical Engineering, 1998).
12. S. Bendersky, N. S. Kopeika, and N. Blaunstein, "Atmospheric optical turbulence over land in middle east coastal environments: prediction modeling and measurements," Appl. Opt. **43**(20), 4070–4079 (2004).
13. J. Libich, J. Perez, S. Zvanovec, Z. Ghassemlooy, R. Nebuloni, and C. Capsoni, "Combined effect of turbulence and aerosol on free-space optical links," Appl. Opt. **56**(2), 336–341 (2017).
14. W. G. Alheadary, K.-H. Park, N. Alfaraj, Y. Guo, E. Stegenburgs, T. K. Ng, B. S. Ooi, and M.-S. Alouini, "Free-space optical channel characterization and experimental validation in a coastal environment," Opt. Express **26**(6), 6614–6628 (2018).
15. Y. Li, W. Zhu, X. Wu, and R. Rao, "Equivalent refractive-index structure constant of non-Kolmogorov turbulence," Opt. Express **23**(18), 23004–23012 (2015).
16. A. Zilberman, E. Golbraikh, and N. S. Kopeika, "Propagation of electromagnetic waves in Kolmogorov and non-Kolmogorov atmospheric turbulence: three-layer altitude model," Appl. Opt. **47**(34), 6385–6391 (2008).
17. G. P. Agrawal, *Fiber-Optical Communication Systems*, 3rd ed. (Wiley, 2002).
18. M. Niu, X. Song, J. Cheng, and J. F. Holzman, "Performance analysis of coherent wireless optical communications with atmospheric turbulence," Opt. Express **20**(6), 6515–6520 (2012).
19. P. Wang, L. Zhang, L. Guo, F. Huang, T. Shang, R. Wang, and Y. Yang, "Average BER of subcarrier intensity modulated free space optical systems over the exponentiated Weibull fading channels," Opt. Express, **22**(17), 20828–20841 (2014).
20. Wolfram Research, http://functions.wolfram.com/06.25.20.0001.01
21. Y. L. Luke, *The Special Functions and Their Approximations, Vol. 1* (Academic Press, 1969).
22. S. Chandrasekhar, *Radiative Transfer*, New York, (Dover, 1960).
23. S. K. Satheesh and K. K. Moorthy, "Radiative effects of natural aerosols: A review," Atmos. Environ. **39**(11), 2089–2110 (2005).
24. S. S. Babu, S. K. Satheesh, and K. K. Moorthy, "Aerosol radiative forcing due to enhanced black carbon at an urban site in India," Geophys. Res. Lett. **29**(18), 27-1–27-4 (2002).
25. K. K. Moorthy, S. K. Satheesh, S. S. Babu, and C. B. S. Dutt, "Integrated campaign for aerosols, gases and radiation budget (ICARB): an overview," J. Earth Syst. Sci. **117**(S1), 243–262 (2008).
26. S. K. Satheesh, K. K. Moorthy, S. S. Babu, V. Vinoj, and C. B. S. Dutt, "Climate implications of large warming by elevated aerosol over India," Geophys. Res. Lett. **35**(19), L19809 (2008).
27. K. N. Liou, An introduction to atmospheric radiation, Vol. 84, (Elsevier, 2002).
28. P. Ricchiazzi, S. Yang, C. Gautier, and D. Sowle, "SBDART, a research and teaching tool for plane-parallel radiative transfer in the Earth's atmosphere," Bull. Am. Meteorol. Soc. **79**(10), 2101–2114 (1998).
29. M. Hess, P. Koepke, and I. Schult, "Optical properties of aerosols and clouds: the software package OPAC," Bull. Am. Meteorol. Soc. **79**(5), 831–844 (1998).